Brief Communications

D1 Receptor Modulation of Action Potential Firing in a Subpopulation of Layer 5 Pyramidal Neurons in the Prefrontal Cortex

Hannah J. Seong and Adam G. Carter
Center for Neural Science, New York University, New York, New York 10003

Dopamine modulation in the prefrontal cortex is important for cognitive processing and disrupted in diverse neuropsychiatric diseases. Activation of D1 receptors is thought to enable working memory by enhancing the firing properties of pyramidal neurons. However, these receptors are only sparsely expressed in the prefrontal cortex, and how they impact individual neurons remains unknown. Here we study D1 receptor modulation of layer 5 pyramidal neurons in acute slices of the mouse prefrontal cortex. Using whole-cell recordings and two-photon microscopy, we show that neurons expressing D1 receptors have unique morphological and physiological properties. We then demonstrate that activation of these receptors selectively enhances the firing of these neurons by signaling via the protein kinase A pathway. This finding of robust D1 receptor modulation in only a subpopulation of neurons has important implications for cognitive function and disease.

Introduction

The prefrontal cortex (PFC) is important for the learning and expression of cognitive behaviors in mammals (Goldman-Rakic, 1995; Miller and Cohen, 2001). Dopamine modulation in the PFC helps generate the persistent neural activity needed for working memory (Seamans and Yang, 2004). Perturbations in dopamine signaling are implicated in diseases ranging from schizophrenia to drug addiction (Knable and Weinberger, 1997; Goldstein and Volkow, 2011). While dopamine can signal through many G-protein-coupled receptors, the D1 subtype is particularly important in the PFC (Sawaguchi and Goldman-Rakic, 1991; Williams and Goldman-Rakic, 1995; Seamans et al., 1998).

D1 receptors signal via α_s subunits to stimulate adenylyl cyclase and activate protein kinase A (PKA), with many downstream targets (Greengard, 2001). Activation of D1 receptors influences the excitability of individual pyramidal neurons (Yang and Seamans, 1996), but it remains unclear whether this is cell-autonomous (Gorelova and Yang, 2000; Dong and White, 2003; Dong et al., 2004) or reflects changes in synaptic activity (Seamans et al., 2001; Wang and O'Donnell, 2001; Chen et al., 2004). Moreover, D1 receptors are sparsely expressed in deep layers of the PFC (Gaspar et al., 1995), where dopaminergic inputs are targeted (Emson and Koob, 1978; Descarries et al., 1987). One possibility is that only a subpopulation of neurons in the PFC expresses D1 receptors, as observed in the striatum (Gerfen et al., 1990). Dopamine could thus influence working memory and other cognitive behaviors by selectively controlling the firing properties of these neurons.

Here we use whole-cell recordings and two-photon microscopy to study D1 receptor modulation of layer 5 (L5) pyramidal neurons in acute slices of the mouse PFC. We use BAC (bacterial artificial chromosome) transgenic animals to show that D1 receptors are found in a minority of neurons that have compact dendrites and exhibit burst firing. We find that the firing properties of these D1-positive (D1+) neurons, in contrast to D1-negative (D1−) neurons, are strongly influenced by activation of D1 receptors signaling through the PKA pathway. These results indicate that D1 receptor modulation is restricted to a subpopulation of neurons in the PFC, with important implications for cognitive function and disease.

Materials and Methods

Slice preparation. L5 pyramidal neurons were studied in acute coronal slices of the medial PFC from male and female hemizygous postnatal day 21–28 BAC D1-tdTomato mice (Shuen et al., 2008) in a Swiss Webster background. Mice were anesthetized with a lethal dose of ketamine and xylazine and perfused intracardially with ice-cold external solution containing (in mM): 65 sucrose, 76 NaCl, 25 $NaHCO_3$, 1.4 NaH_2PO_4, 25 glucose, 2.5 KCl, 1 $CaCl_2$, 5 $MgCl_2$, 0.4 Na-ascorbate, and 2 Na-pyruvate (295–305 mOsm), bubbled with 95% O_2/5% CO_2. Coronal slices (300 μm thick) were cut in ice-cold external solution and transferred to ACSF containing (in mM): 120 NaCl, 25 $NaHCO_3$, 1.4 NaH_2PO_4, 21 glucose, 2.5 KCl, 2 $CaCl_2$, 1 $MgCl_2$, 0.4 Na-ascorbate, and 2 Na-pyruvate (295–305 mOsm), bubbled with 95% O_2/5% CO_2. After 30 min in ACSF at 35°C, slices were allowed to recover for 30 min at 24°C. All experiments were conducted at near-physiological temperatures (32−34°C). All chemicals were from Sigma.

Electrophysiology. Whole-cell current-clamp recordings were obtained from L5 pyramidal neurons located 450–550 μm from the pia.

Received March 20, 2012; revised June 12, 2012; accepted June 18, 2012.

Author contributions: H.J.S. and A.G.C. designed research; H.J.S. performed research; H.J.S. analyzed data; H.J.S. and A.G.C. wrote the paper.

This work was supported by NIH Grants 5T32 MH019524 (H.J.S.) and R01 MH085974 (A.G.C.). We thank members of the Carter laboratory, Michael Beierlein, and Anatol Kreitzer for helpful discussions and comments on the manuscript. We thank John Cassel for technical assistance.

The authors declare no competing financial interests.

Correspondence should be addressed to Adam G. Carter at the above address. E-mail: adam.carter@nyu.edu.

DOI:10.1523/JNEUROSCI.1367-12.2012

 0270-6474/12/3210516-06$15.00/0

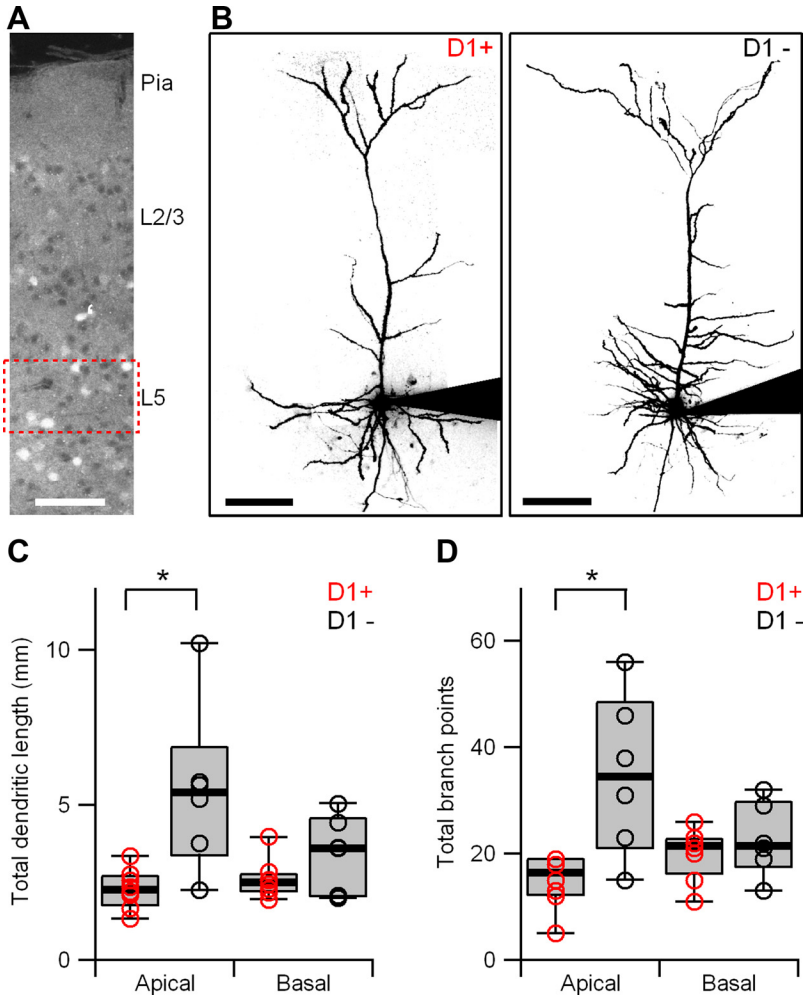

Figure 1. Morphological properties of D1+ neurons. ***A***, Confocal image of a coronal slice containing the PFC. Dashed box shows where L5 pyramidal neurons were recorded. Scale bar, 100 μm. ***B***, Two-photon image stacks of D1+ (left) and D1− (right) L5 pyramidal neurons. Recording pipettes are indicated by solid triangles for clarity. Scale bars, 100 μm. ***C***, Summary of total dendritic length in the apical and basal dendrites of D1+ (red) and D1− (black) neurons. ***D***, Summary of total branch points in the apical and basal dendrites of D1+ (red) and D1− (black) neurons. Significance is indicated by $*p < 0.05$.

D1+ neurons were identified by their fluorescently labeled cell bodies and targeted with IR-DIC. Borosilicate recording pipettes (3–4 MΩ) were filled with the following (in mM): 135 K-gluconate, 7 KCl, 10 HEPES, 10 Na-phosphocreatine, 4 Mg_2-ATP, and 0.4 NaGTP (290–300 mOsm, pH 7.3 with KOH). The internal solution also contained 30 μM Alexa-594 to image neuronal morphology and 200 μM Fluo-5F. For high-resolution image stacks, neurons were filled via the patch pipette for at least 20 min before imaging. Recordings were made using a Multiclamp 700B amplifier. Recordings were not corrected for the liquid junction potential. All experiments were performed in the presence of the following synaptic blockers (in μM): 10 NBQX, 10 (*R*)-CPP, 10 SR-95531. D1 receptor agonists SKF-38393 and SKF-81297 and D1 receptor antagonist SCH-23390 were made up in water and protected from light. The agonists were allowed to wash-in for 5 min before data acquisition. In some experiments, the internal solution contained 3 mM GDP-βS, 100 μM PKA inhibitor fragment (6–22) (PKI), or 100 μM PKC inhibitor fragment (19–36) (PKC-I). All chemicals were from Sigma or Tocris Bioscience, with the exception of PKC-I (EMD Chemicals).

Two-photon microscopy. Two-photon imaging was performed using a custom microscope, as previously described (Chalifoux and Carter, 2010). At the end of each experiment, a high-resolution image stack ($\Delta x = 0.5$ μm, $\Delta y = 0.5$ μm, $\Delta z = 1$ μm) was taken of the recorded neuron for morphology analysis. Three-dimensional reconstructions were performed using NeuronStudio (Wearne et al., 2005). Sholl analysis reveals the number of branch points between increasing three-dimensional spheres emanating from the soma. Image stacks in Figure 1 were processed with a 2-pixel diameter median filter for display purposes.

Histology and confocal microscopy. Mice were deeply anesthetized and perfused intracardially as described above. Brains were removed, transferred to a solution containing 4% paraformaldehyde in 0.01 M PBS, and fixed for 24 h at 4°C. Coronal sections (70 μm thick) were cut in PBS, placed on gelatin-coated microscope slides, and sealed under glass coverslips using ProLong Gold antifade reagent with DAPI mounting media (Invitrogen). Images were acquired with a Leica TCX SP5 confocal microscope using a 40× objective and excitation wavelength of 561 nm. Montages were stitched using the mosaicJ plugin in ImageJ (NIH).

Data acquisition and analysis. Electrophysiology and two-photon imaging data were acquired using National Instruments boards and custom software written in Matlab (MathWorks). Off-line analysis was performed using custom routines written in Igor Pro (WaveMetrics). Summary data are shown as box plots, with individual data points (open circles), median (thick line), interquartile range (box), and 10–90% range (whiskers). Summary data reported in the text are the arithmetic mean ± SEM. There are occasionally small differences between the median and mean, which explains some discrepancies between values shown in figures and reported in the text. Significance was defined as $p < 0.05$ and determined using the nonparametric Wilcoxon–Mann–Whitney two-sample rank test or the Wilcoxon signed rank test for paired data (when appropriate), neither of which makes assumptions about the data distribution. In Figure 2, input resistance and voltage sag were quantified from the response to a hyperpolarizing current pulse (−50 pA, 500 ms). Input resistance was calculated using the difference between resting potential and steady-state response to the pulse. Voltage sag was calculated as the difference between maximum hyperpolarization and steady-state response, normalized to the maximum hyperpolarization. Burst firing was quantified as the ratio of the interspike intervals (ISIs) of the first and last pairs of action potentials during a train of five action potentials. Changes in firing (ΔAP) were calculated as the difference in the number of evoked action potentials. Representative traces in Figures 2, 3, and 4 were baseline subtracted for display purposes.

Results

Morphological properties

We examined the properties of L5 pyramidal neurons expressing D1 receptors in acute slices of mouse PFC. To distinguish between D1+ and D1− neurons, we used BAC transgenic animals expressing tdTomato from the D1 promoter (Shuen et al., 2008). We found that D1+ neurons were interspersed throughout the PFC, in agreement with sparse D1 receptor mRNA expression (Gaspar et al., 1995; Fig. 1*A*). However, these neurons were concentrated in deep layers, consistent with high levels of dopaminergic fibers in this region (Emson and Koob, 1978; Descarries et al., 1987).

We used whole-cell recordings to introduce fluorescent dyes into D1+ and D1− L5 pyramidal neurons and two-photon mi-

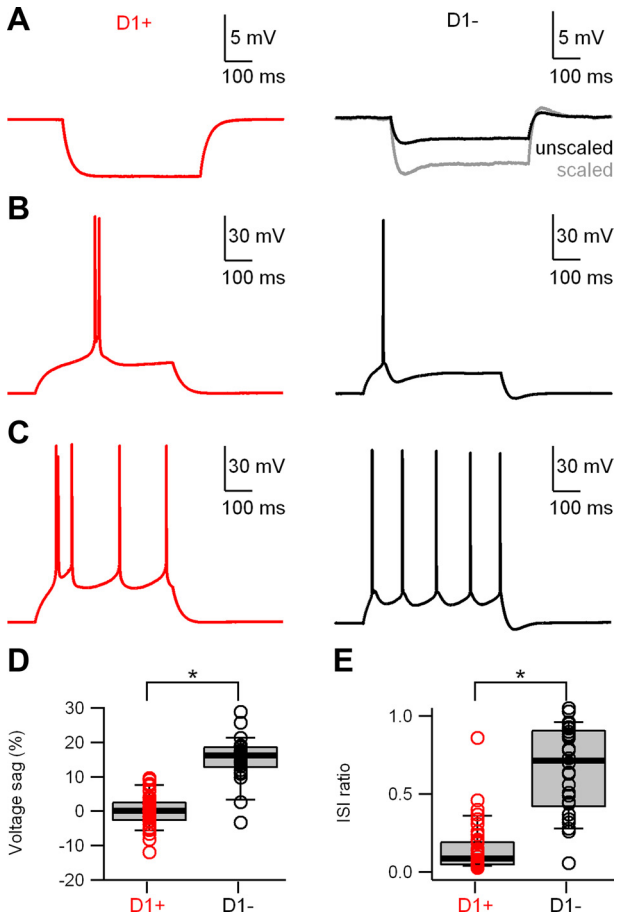

Figure 2. Physiological properties of D1+ neurons. ***A***, Representative traces from D1+ (left, red) and D1− (right, black) L5 pyramidal neurons in response to a hyperpolarizing current step. The peak response of the D1− neuron is scaled to that of the D1+ neuron for comparison (gray). ***B***, Similar to ***A***, but in response to a minimal depolarizing current step (AP_1). ***C***, Similar to ***B***, but in response to a larger current step (AP_2). ***D***, Summary of voltage sag in D1+ (red) and D1− (black) neurons. ***E***, Summary of ratio of first and last ISIs in response to the larger current step (AP_2) in D1+ (red) and D1− (black) neurons. Note that representative traces are baseline subtracted for display purposes. Significance is indicated by $*p < 0.05$.

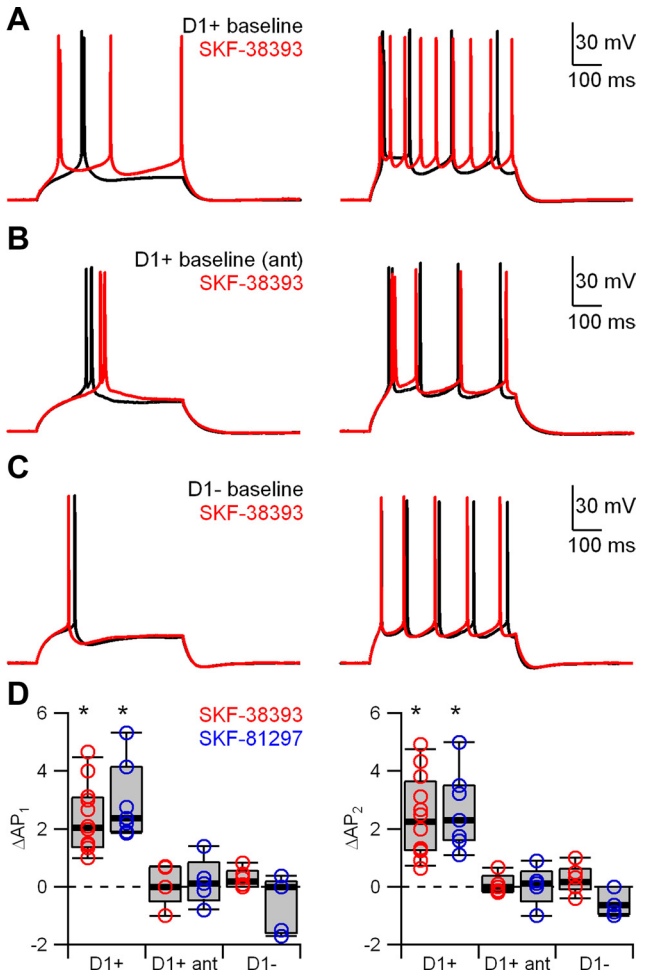

Figure 3. D1 receptor modulation of firing properties. ***A***, Representative traces from a D1+ L5 pyramidal neuron in response to a minimal depolarizing current step (AP_1, left) and larger current step (AP_2, right) under baseline conditions (black) and after bath application of the D1 receptor agonist SKF-38393 (red). ***B***, Similar to ***A***, but in the presence of the D1 receptor antagonist SCH-23390 (ant). ***C***, Similar to ***A***, but from a D1− neuron. ***D***, Summary of changes in firing in response to the minimal current step (ΔAP_1, left) and larger current step (ΔAP_2, right), after bath application of SKF-38393 (red) or SKF-81297 (blue). Significant difference from baseline conditions is indicated by $*p < 0.05$.

croscopy to view their morphology (Fig. 1*B*). Using high-resolution three-dimensional reconstructions (see Materials and Methods), we found that the apical dendrites of D1+ neurons were smaller and less complex than D1− neurons. Total dendritic length was less in the apical dendrites (D1+ = 2.3 ± 0.2 mm, $n = 8$; D1− = 5.5 ± 1.1 mm, $n = 6$; $p = 0.008$), while the basal dendrites were similar (D1+ = 2.6 ± 0.2 mm; D1− = 3.5 ± 0.5 mm; $p = 0.35$; Fig. 1*C*). Sholl analysis also revealed substantially fewer total dendritic branch points in the apical dendrites (D1+ = 15 ± 2; D1− = 35 ± 6; $p = 0.008$), while the basal dendrites were again comparable (D1+ = 20 ± 2; D1− = 23 ± 3; $p = 0.68$; Fig. 1*D*). These results indicate that L5 pyramidal neurons expressing D1 receptors represent a morphologically distinct set of cells in the PFC.

Electrophysiological properties

L5 pyramidal neurons in the PFC are a heterogeneous population whose physiological properties can vary widely (Kawaguchi, 1993; Yang et al., 1996). Using current-clamp recordings, we next examined the membrane properties of D1+ and D1− L5 pyramidal neurons (Fig. 2*A*). We found that the resting potential was more hyperpolarized in D1+ neurons (V_m: D1+ = −74 ± 1 mV, $n = 44$; D1− = −68 ± 1 mV, $n = 30$; $p = 1 \times 10^{-6}$). In response to hyperpolarizing current injections from rest, we found that the input resistance of these neurons was also significantly higher (R_{in}: D1+ = 189 ± 11 MΩ; D1− = 87 ± 6 MΩ; $p = 1 \times 10^{-9}$) (see Materials and Methods). These recordings also revealed an absence of the depolarizing voltage sag, which reflects activation of hyperpolarization-activated channels and is a canonical feature of most L5 pyramidal neurons (Robinson and Siegelbaum, 2003). The hyperpolarization-evoked voltage sag was significantly smaller in D1+ neurons (sag: D1+ = 0.3 ± 0.7%; D1− = 15 ± 1%; $p = 3 \times 10^{-11}$) (see Materials and Methods; Fig. 2*D*). These results show that D1+ neurons have unique membrane properties, further indicating that they represent a distinct subpopulation of cells in the PFC.

We next examined the firing properties of D1+ and D1− L5 pyramidal neurons in response to depolarizing current injections from rest. For these experiments, we evoked a minimal number of action potentials (AP_1; Fig. 2*B*) or a train of five action potentials (AP_2; Fig. 2*C*). We found that D1− neurons fired regularly, as observed in many L5 pyramidal neurons throughout the cor-

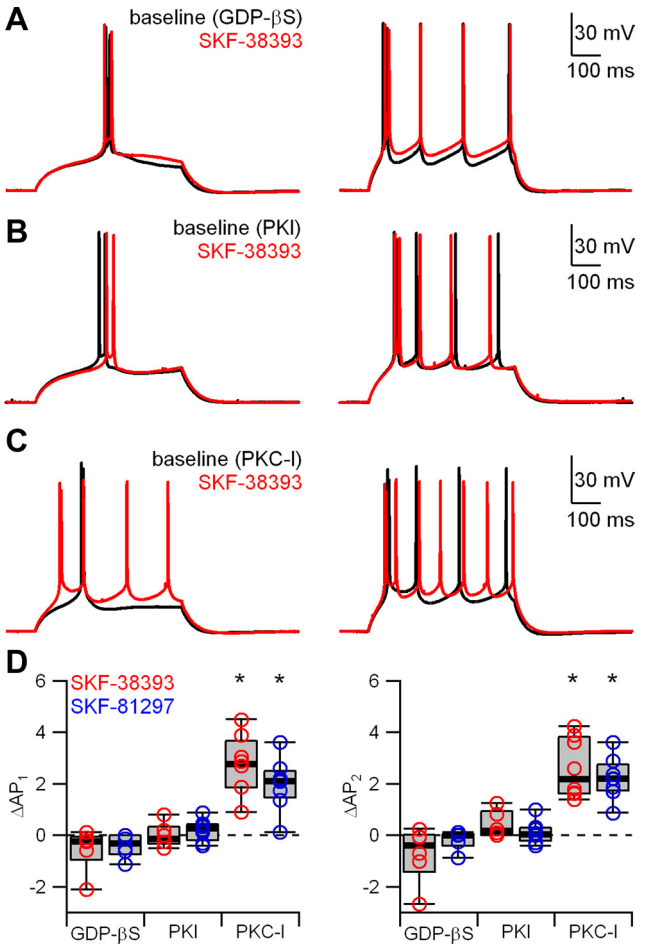

Figure 4. Dependence on the PKA pathway. ***A***, Representative traces from a D1+ L5 pyramidal neuron patched with GDP-βS internal in response to a minimal depolarizing current step (AP_1, left) and larger current step (AP_2, right) under baseline conditions (black) and after bath application of SKF-38393 (red). ***B***, Similar to ***A***, but from a D1+ neuron patched with PKI internal. ***C***, Similar to ***A***, but from a D1+ neuron patched with PKC-I internal. ***D***, Summary of changes in firing in response to the minimal current step (ΔAP_1, left) and larger current step (ΔAP_2, right), after bath application of SKF-38393 (red) or SKF-81297 (blue). Significant difference from baseline conditions is indicated by $^*p < 0.05$.

tex. In contrast, D1+ neurons fired brief bursts of action potentials, even in response to minimal current injections. The ISI of the first two action potentials during AP_2 was significantly shorter in D1+ neurons (ISI: D1+ = 18 ± 3 ms, D1− = 76 ± 5 ms, $p = 1 \times 10^{-11}$). We quantified bursting as the ratio of the ISI of the first and last pairs of action potentials during AP_2, which was significantly lower in D1+ neurons (ISI ratio: D1+ = 0.15 ± 0.02; D1− = 0.66 ± 0.05; $p = 2 \times 10^{-10}$) (see Materials and Methods; Fig. 2*E*). The observed differences in input resistance, voltage sag and firing properties were similar when D1+ neurons were depolarized to −65 mV or D1− neurons hyperpolarized to −75 mV (data not shown). Finally, applying ZD-7288 (10 μM) to block hyperpolarization-activated channels reduced the resting potential of D1− neurons ($V_{m\ (ZD)} = -79 \pm 2$ mV, $n = 11$; $\Delta V_m = -10 \pm 1$ mV, $p = 0.001$) and eliminated their voltage sag ($sag_{(ZD)} = 0.6 \pm 1.8\%$; $\Delta sag = -13 \pm 1\%$, $p = 1 \times 10^{-4}$) but only slightly increased their input resistance ($R_{in(ZD)} = 111 \pm 13$ MΩ; $\Delta R_{in} = 33 \pm 11\%$, $p = 0.002$) and did not generate burst firing ($ISI_{(ZD)} = 84 \pm 13$ ms, $p = 0.97$; ISI $ratio_{(ZD)} = 0.72 \pm 0.08$, $p = 0.9$). Together, these results indicate that L5 pyramidal neurons expressing D1 receptors also have unique physiological properties.

D1 receptor modulation

We next assessed how D1 receptor activation modulates the firing properties of these two classes of neurons. To assess cell-autonomous effects, all experiments were performed in the presence of blockers for both excitatory and inhibitory synaptic transmission (see Materials and Methods). We first obtained stable responses to depolarizing current injections that evoked a minimal number of action potentials (AP_1) or a train of five action potentials (AP_2). We then washed in the selective D1 receptor agonist SKF-38393 (30 μM) and assessed the impact on firing. In D1+ neurons, we found that the number of action potentials greatly increased in response to D1 receptor activation ($\Delta AP_1 = 2.3 \pm 0.3$, $p = 5 \times 10^{-4}$; $\Delta AP_2 = 2.4 \pm 0.4$, $p = 5 \times 10^{-4}$; $n = 12$) (see Materials and Methods; Fig. 3*A*). This modulation was completely blocked by the presence of the D1 receptor antagonist SCH-23390 (10 μM) ($\Delta AP_1 = 0.1 \pm 0.3$, $p = 1$; $\Delta AP_2 = 0.1 \pm 0.2$, $p = 1$; $n = 5$; Fig. 3*B*). In contrast, D1 receptor activation had no effect on the firing of D1− neurons in the same animals ($\Delta AP_1 = 0.3 \pm 0.1$, $p = 0.13$; $\Delta AP_2 = 0.2 \pm 0.2$, $p = 0.38$; $n = 6$; Fig. 3*C*). We observed similar effects with the alternative D1 receptor agonist SKF-81297 (10 μM), which also increased firing in D1+ neurons ($\Delta AP_1 = 2.8 \pm 0.4$, $p = 0.004$; $\Delta AP_2 = 2.5 \pm 0.4$, $p = 0.004$; $n = 9$), had no effect in the presence of SCH-23390 ($\Delta AP_1 = 0.2 \pm 0.4$, $p = 0.63$; $\Delta AP_2 = 0.1 \pm 0.3$, $p = 0.88$; $n = 5$), and had no effect in D1− neurons ($\Delta AP_1 = -0.6 \pm 0.4$, $p = 0.5$; $\Delta AP_2 = -0.5 \pm 0.2$, $p = 0.25$; $n = 5$; Fig. 3*D*). These results indicate that the expression of functional D1 receptors is restricted to D1+ neurons, and strongly enhance their firing properties when activated.

In addition to this increased firing, we found that activation of D1 receptors caused a small but significant depolarization of D1+ neurons (SKF-38393: $\Delta V_m = 7.6 \pm 2.1$ mV, $p = 0.002$; SKF-81297: $\Delta V_m = 2.5 \pm 0.8$ mV, $p = 0.03$). Activation of these receptors also caused a small increase in the input resistance of D1+ neurons (SKF-38393: $\Delta R_{in} = 12 \pm 3\%$, $p = 0.03$; SKF-81297: $\Delta R_{in} = 21 \pm 5\%$, $p = 0.004$). Both of these effects were blocked by the D1 antagonist SCH-23390 (10 μM) and were absent in D1− neurons (data not shown), suggesting they are also due to selective activation of D1 receptors.

Dependence on the PKA pathway

D1 receptors are usually thought to signal through α_s subunits to activate adenylyl cyclase and stimulate PKA (Greengard, 2001). Activation of this pathway has many downstream effects that could influence the firing properties of pyramidal neurons (Seamans and Yang, 2004). However, the protein kinase C (PKC) pathway could also contribute to D1 receptor modulation in the PFC (Young and Yang, 2004; Chen et al., 2007). We next assessed the involvement of these two signaling pathways in D1 receptor modulation of D1+ L5 pyramidal neurons. We first examined the impact of blocking all G-protein signaling by including GDP-βS (3 mM) in the internal solution. We found that GDP-βS eliminated the increase in firing due to both SKF-38393 ($\Delta AP_1 = -0.5 \pm 0.3$, $p = 0.09$; $\Delta AP_2 = -0.7 \pm 0.4$, $p = 0.16$; $n = 6$; Fig. 4*A*) and SKF-81297 ($\Delta AP_1 = -0.4 \pm 0.2$, $p = 0.13$; $\Delta AP_2 = -0.2 \pm 0.2$, $p = 0.63$; $n = 6$; Fig. 4*D*), confirming that G-protein signaling cascades are involved. We then determined the impact of specifically eliminating PKA activity by including PKI (100 μM) in the internal solution. We found that PKI also blocked the effects of both SKF-38393 ($\Delta AP_1 = 0.0 \pm 0.2$, $p = 0.75$; $\Delta AP_2 = 0.4 \pm 0.2$, $p = 0.13$; $n = 6$; Fig. 4*B*) and SKF-81297 ($\Delta AP_1 = 0.2 \pm 0.2$, $p = 0.25$; $\Delta AP_2 = 0.1 \pm 0.2$, $p = 0.69$; $n = 8$; Fig. 4*D*), verifying that PKA signaling is also engaged. In contrast, we

found that including PKC-I (100 μM) in the internal solution did not prevent the effects of either SKF-38393 ($\Delta AP_1 = 2.7 \pm 0.4$, $p = 0.008$; $\Delta AP_2 = 2.6 \pm 0.4$, $p = 0.008$; $n = 8$; Fig. 4*C*) or SKF-81297 ($\Delta AP_1 = 2.0 \pm 0.4$, $p = 0.008$; $\Delta AP_2 = 2.2 \pm 0.3$, $p = 0.008$; $n = 8$; Fig. 4*D*), indicating that PKC signaling is not required. Together, these results indicate that D1 receptors signal through the PKA pathway to influence the firing properties of D1+ neurons.

Discussion

We have used whole-cell recordings and two-photon microscopy to study the properties of L5 pyramidal neurons expressing D1 receptors in acute slices of the mouse PFC. We first showed that D1 receptors are found in a subpopulation of neurons that have relatively compact dendrites and undergo burst firing. We then determined that activation of D1 receptors selectively enhances the firing properties of these neurons by signaling through the PKA pathway. These results expand our understanding of dopamine modulation in the PFC, with important implications for cognitive function and disease.

The mammalian PFC plays a critical role in the learning and expression of cognitive behaviors (Goldman-Rakic, 1995; Miller and Cohen, 2001). Activation of D1 receptors in the PFC helps generate the persistent neural activity needed for working memory (Sawaguchi and Goldman-Rakic, 1991; Williams and Goldman-Rakic, 1995). These receptors have been shown to influence the excitability of individual pyramidal neurons (Yang and Seamans, 1996). However, it has been difficult to determine whether this effect is cell-autonomous (Gorelova and Yang, 2000; Dong and White, 2003; Dong and White, 2004) or reflects changes in synaptic activity (Seamans et al., 2001; Wang and O'Donnell, 2001; Chen et al., 2004). While heightened synaptic responses are involved in generating persistent activity (Wang, 1999; Durstewitz et al., 2000), our findings indicate that D1 receptors can also directly influence the firing properties of L5 pyramidal neurons in the PFC. Moreover, our results indicate that this modulation only occurs in a subpopulation of neurons expressing these receptors.

While D1 receptors are clearly important for PFC function, they are only sparsely expressed in deep layers (Gaspar et al., 1995). To identify D1+ L5 pyramidal neurons, we took advantage of BAC transgenic animals expressing tdTomato from the D1 promoter (Shuen et al., 2008). This approach has previously been used to identify different classes of medium spiny neurons in the striatum (Gong et al., 2003). Recently, it has also been used to identify a subpopulation of pyramidal neurons expressing D2 receptor in the PFC (Gee et al., 2012). In our study, we found that D1+ neurons in the PFC have more negative resting potentials, higher input resistances, and undergo burst firing. Our two-photon reconstructions also revealed that D1+ neurons have smaller and less complex apical dendrites. These properties contrast with D1− neurons, but are similar to other subpopulations of L5 pyramidal neurons in the PFC (Kawaguchi, 1993; Yang et al., 1996) that have unique projection targets (Morishima and Kawaguchi, 2006; Dembrow et al., 2010; Morishima et al., 2011; Gee et al., 2012). One interesting possibility is that D1+ neurons also make distinct connections onto other neurons in the local circuit. This could support the recurrent excitation required for the persistent activity thought to underlie working memory (Goldman-Rakic, 1995; Miller and Cohen, 2001). In the future, it will be important to explore the connectivity of different subpopulations of pyramidal neurons in their local and long-range circuits.

Once we identified a subpopulation of D1+ neurons, we used pharmacology to assess how D1 receptors affected their firing properties. We found that two widely used agonists of D1 receptors both strongly enhanced the firing of these neurons. This effect was highly selective, as it was blocked by D1 receptor antagonists, and not present in D1− neurons. D1 receptors are G-protein-coupled receptors that activate PKA to modulate diverse downstream targets (Greengard, 2001). We found that D1 receptor modulation was eliminated by intracellular blockade of the PKA pathway, consistent with previous studies (Seamans and Yang, 2004). In contrast, this modulation was not affected by intracellular blockade of the PKC pathway, which can also be activated by these receptors (Young and Yang, 2004; Chen et al., 2007). While the targets of the PKA pathway remain unknown, possibilities include inhibition of K channels (Dong and White, 2003; Dong et al., 2004) and activation of Na channels (Gorelova and Yang, 2000). Previous studies on D1 receptor modulation in the PFC have considered a mixed population, likely consisting of both D1+ and D1− neurons. In the future, it will be interesting to determine the biophysical mechanisms responsible for modulation in identified D1+ neurons.

Finally, dysfunctional dopamine modulation in the PFC is prevalent in neuropsychiatric diseases ranging from drug addiction (Goldstein and Volkow, 2011) to schizophrenia (Knable and Weinberger, 1997). For example, excess D1 receptor activation has been linked to behavioral sensitization to drugs of abuse such as cocaine (Sorg et al., 2001). In contrast, reduced D1 receptor activation has been implicated in the symptoms of schizophrenia (Abi-Dargham and Moore, 2003). Our results indicate that D1 receptors are present in only a select subpopulation of L5 pyramidal neurons. Understanding how these neurons participate in their larger circuits may ultimately elucidate the role of dopamine in both normal cognitive function and disease.

References

Abi-Dargham A, Moore H (2003) Prefrontal DA transmission at D1 receptors and the pathology of schizophrenia. Neuroscientist 9:404–416.

Chalifoux JR, Carter AG (2010) GABAB receptors modulate NMDA receptor calcium signals in dendritic spines. Neuron 66:101–113.

Chen G, Greengard P, Yan Z (2004) Potentiation of NMDA receptor currents by dopamine D1 receptors in prefrontal cortex. Proc Natl Acad Sci U S A 101:2596–2600.

Chen L, Bohanick JD, Nishihara M, Seamans JK, Yang CR (2007) Dopamine D1/5 receptor-mediated long-term potentiation of intrinsic excitability in rat prefrontal cortical neurons: Ca^{2+}-dependent intracellular signaling. J Neurophysiol 97:2448–2464.

Dembrow NC, Chitwood RA, Johnston D (2010) Projection-specific neuromodulation of medial prefrontal cortex neurons. J Neurosci 30:16922–16937.

Descarries L, Lemay B, Doucet G, Berger B (1987) Regional and laminar density of the dopamine innervation in adult rat cerebral cortex. Neuroscience 21:807–824.

Dong Y, White FJ (2003) Dopamine D1-class receptors selectively modulate a slowly inactivating potassium current in rat medial prefrontal cortex pyramidal neurons. J Neurosci 23:2686–2695.

Dong Y, Cooper D, Nasif F, Hu XT, White FJ (2004) Dopamine modulates inwardly rectifying potassium currents in medial prefrontal cortex pyramidal neurons. J Neurosci 24:3077–3085.

Durstewitz D, Seamans JK, Sejnowski TJ (2000) Dopamine-mediated stabilization of delay-period activity in a network model of prefrontal cortex. J Neurophysiol 83:1733–1750.

Emson PC, Koob GF (1978) The origin and distribution of dopamine-containing afferents to the rat frontal cortex. Brain Res 142:249–267.

Gaspar P, Bloch B, Le Moine C (1995) D1 and D2 receptor gene expression in the rat frontal cortex: cellular localization in different classes of efferent neurons. Eur J Neurosci 7:1050–1063.

Gee S, Ellwood I, Patel T, Luongo F, Deisseroth K, Sohal VS (2012) Synaptic

activity unmasks dopamine d2 receptor modulation of a specific class of layer v pyramidal neurons in prefrontal cortex. J Neurosci 32:4959–4971.
Gerfen CR, Engber TM, Mahan LC, Susel Z, Chase TN, Monsma FJ Jr, Sibley DR (1990) D1 and D2 dopamine receptor-regulated gene expression of striatonigral and striatopallidal neurons. Science 250:1429–1432.
Goldman-Rakic PS (1995) Cellular basis of working memory. Neuron 14:477–485.
Goldstein RZ, Volkow ND (2011) Dysfunction of the prefrontal cortex in addiction: neuroimaging findings and clinical implications. Nat Rev Neurosci 12:652–669.
Gong S, Zheng C, Doughty ML, Losos K, Didkovsky N, Schambra UB, Nowak NJ, Joyner A, Leblanc G, Hatten ME, Heintz N (2003) A gene expression atlas of the central nervous system based on bacterial artificial chromosomes. Nature 425:917–925.
Gorelova NA, Yang CR (2000) Dopamine D1/D5 receptor activation modulates a persistent sodium current in rat prefrontal cortical neurons in vitro. J Neurophysiol 84:75–87.
Greengard P (2001) The neurobiology of dopamine signaling. Biosci Rep 21:247–269.
Kawaguchi Y (1993) Groupings of nonpyramidal and pyramidal cells with specific physiological and morphological characteristics in rat frontal cortex. J Neurophysiol 69:416–431.
Knable MB, Weinberger DR (1997) Dopamine, the prefrontal cortex and schizophrenia. J Psychopharmacol 11:123–131.
Miller EK, Cohen JD (2001) An integrative theory of prefrontal cortex function. Annu Rev Neurosci 24:167–202.
Morishima M, Kawaguchi Y (2006) Recurrent connection patterns of corticostriatal pyramidal cells in frontal cortex. J Neurosci 26:4394–4405.
Morishima M, Morita K, Kubota Y, Kawaguchi Y (2011) Highly differentiated projection-specific cortical subnetworks. J Neurosci 31:10380–10391.
Robinson RB, Siegelbaum SA (2003) Hyperpolarization-activated cation currents: from molecules to physiological function. Annu Rev Physiol 65:453–480.
Sawaguchi T, Goldman-Rakic PS (1991) D1 dopamine receptors in prefrontal cortex: involvement in working memory. Science 251:947–950.
Seamans JK, Yang CR (2004) The principal features and mechanisms of dopamine modulation in the prefrontal cortex. Prog Neurobiol 74:1–58.
Seamans JK, Floresco SB, Phillips AG (1998) D1 receptor modulation of hippocampal-prefrontal cortical circuits integrating spatial memory with executive functions in the rat. J Neurosci 18:1613–1621.
Seamans JK, Durstewitz D, Christie BR, Stevens CF, Sejnowski TJ (2001) Dopamine D1/D5 receptor modulation of excitatory synaptic inputs to layer V prefrontal cortex neurons. Proc Natl Acad Sci U S A 98:301–306.
Shuen JA, Chen M, Gloss B, Calakos N (2008) Drd1a-tdTomato BAC transgenic mice for simultaneous visualization of medium spiny neurons in the direct and indirect pathways of the basal ganglia. J Neurosci 28:2681–2685.
Sorg BA, Li N, Wu WR (2001) Dopamine D1 receptor activation in the medial prefrontal cortex prevents the expression of cocaine sensitization. J Pharmacol Exp Ther 297:501–508.
Wang J, O'Donnell P (2001) D(1) dopamine receptors potentiate NMDA-mediated excitability increase in layer V prefrontal cortical pyramidal neurons. Cereb Cortex 11:452–462.
Wang XJ (1999) Synaptic basis of cortical persistent activity: the importance of NMDA receptors to working memory. J Neurosci 19:9587–9603.
Wearne SL, Rodriguez A, Ehlenberger DB, Rocher AB, Henderson SC, Hof PR (2005) New techniques for imaging, digitization and analysis of three-dimensional neural morphology on multiple scales. Neuroscience 136:661–680.
Williams GV, Goldman-Rakic PS (1995) Modulation of memory fields by dopamine D1 receptors in prefrontal cortex. Nature 376:572–575.
Yang CR, Seamans JK (1996) Dopamine D1 receptor actions in layers V-VI rat prefrontal cortex neurons in vitro: modulation of dendritic-somatic signal integration. J Neurosci 16:1922–1935.
Yang CR, Seamans JK, Gorelova N (1996) Electrophysiological and morphological properties of layers V-VI principal pyramidal cells in rat prefrontal cortex in vitro. J Neurosci 16:1904–1921.
Young CE, Yang CR (2004) Dopamine D1/D5 receptor modulates state-dependent switching of soma-dendritic Ca^{2+} potentials via differential protein kinase A and C activation in rat prefrontal cortical neurons. J Neurosci 24:8–23.